Green Tea Polyphenols Promote Functional Recovery from Peripheral Nerve Injury in Rats

Authors' Contribution:
Study Design A
Data Collection B
Statistical Analysis C
Data Interpretation D
Manuscript Preparation E
Literature Search F
Funds Collection G

ABCDF 1 Jinhong Chen*
ABCDF 1 Rongyuan Yang*
BCD 1 Honghan Li
ACDEF 2 Jie Lao

1 Department of Orthopedics, Zhangzhou Affiliated Hospital of Fujian Medical University, Zhangzhou, Fujian, P.R. China
2 Department of Hand Surgery, Huashan Affiliated Hospital of Fudan University, Shanghai, P.R. China

Corresponding Author:
Source of support:

* Jinhong Chen and Rongyuan Yang contributed equally
Jie Lao, e-mail: laojiehsah@163.com
Departmental sources

Background:
Peripheral nerve injury (PNI) is a common and progressive disorder with sensory and motor deficits in the peripheral nervous system (PNS). Treatment is difficult, with unfavorable prognosis. Green tea polyphenols (GTPs) exert neuroprotective effects on regeneration of the central nervous system (CNS). However, the effects of GTPs on functional recovery of the PNS have not been fully characterized. Consequently, the present study investigated the effects of GTPs on nerve regeneration of rats with PNI.

Material/Methods:
The model of PNI was established in rats by sciatic nerve injury (SNI). Adult male Wistar rats with SNI were randomly divided into a vehicle group and a GTPs group. The compound muscle action potential (CMAP) of rat sciatic nerves (SN) was measured using the CM6240 physiological signal acquisition and processing system. The wet weight of the triceps muscle was determined using an analytical balance. The number of myelinated nerve fibers was counted under an optical microscope. Ultrastructure of the regenerated nerves in SN was observed by transmission electron microscopy. The mRNA and protein expression of nerve growth factor (NGF), growth-associated protein-43 (GAP-43), neurofilament 200 (NF200), and myelin-associated glycoprotein (MAG) in SN stumps were measured by real-time quantification PCR (RT-qPCR) and Western blot, respectively.

Results:
In rats with SNI, GTPs relieved the adhesion between nerve anastomosis and surrounding tissues, and significantly increased nerve conduction velocity, wet weight of the triceps muscle, and development and axonal regeneration of myelinated nerve fibers. Moreover, GTPs promoted the mRNA and protein expressions of NGF, GAP-43, NF200, and MAG in SN stumps.

Conclusions:
GTPs promotes nerve regeneration in rats with SNI.

MeSH Keywords:
Medicine, Chinese Traditional • Nerve Regeneration • Peripheral Nerve Injuries

Full-text PDF:
https://www.medscimonit.com/abstract/index/idArt/923806

📄 2944   📊 4   📈 5   📖 38

Background

The PNS, which links the CNS (spinal cord and brain) and the rest of body, is fragile and easily damaged. PNI, which results from trauma or acute compression, accounts for approximately 1.5–4.0% of the world's annual new trauma cases [1]. Nerve regeneration in PNI depends on recovery of limb function, and the nerve growth rate is a key factor in muscular atrophy [2]. Currently, there is no effective therapy for repair of PNI or prevention of muscle atrophy and treatment for nerve regeneration after PNI.

Numerous scholars have explored various treatments for PNI repair, and showed protective effects on nerve regeneration. For instance, laser phototherapy restores denervated muscle atrophy and promotes nerve regeneration of PNI [3], neural conduit is applied for PNI repair [4], 4-aminopyridine (4-AP) promotes recovery of acute PNI and myelin regeneration in rats [2], and vitamin supplements are beneficial for nerve regeneration in acute PNI [5]. However, adverse effects exist, and an accessible, convenient method without adverse effects is urgently needed.

GTPs, the major bioactive compounds of green tea, exert various functions, with anti-oxidation [6], anti-inflammation [7], and anti-cancer [8] effects. In addition, GTPs exhibit protective effects in the CNS. For instance, GTPs stabilize mitochondria in brain neurodegenerative diseases via antioxidants [9], and GTPs alleviate nerve damage after focal cerebral ischemia [10]. However, the effects of GTPs in the PNS have not been investigated. Therefore, the present study was performed to assess the effects of GTPs in the PNS and to lay a theoretical foundation for clinical application of GTPs.

Material and Methods

Animals

Adult male Wistar rats weighing about 170–190 g were purchased from the Laboratory Animal Center of Fujian Medical University (Fuzhou, China). Rats were kept in stable conditions of 22±3°C, 55% relative humidity, and 12-h light/dark cycle with food/water ad libitum. Animal care and procedures were approved by the Animal Use and Care Committee of Huashan Affiliated Hospital of Fudan University, and the study was performed strictly following the guidelines.

Establishment of SNI model in rats

After intraperitoneal injection of 10% chloral hydrate (0.5 ml/100 g) into each rat, a longitudinal incision (2.5 cm in length) was made in the posterior part of the right lower limb femur. Under an operating microscope (Carl Zeiss, Germany), the muscular membranes were cut from the gap between the semitendinosus, semimembranosus, and biceps femoris. By the suspension method, the gluteus maximus muscle was stretched, and the SN was fully exposed. The SN was cut with a sterile blade 0.8 cm below the lower edge of the piriformis muscle, and the wound was sutured with aseptic 11-0 noninvasive nylon thread, while the epineurium was sutured with 4-6 needles. Subsequently, the incision was closed layer-by-layer with sterile 1-0 suture. A microsuture was placed on the epineurium of the anastomosis and served as a marker.

Groups

Adult male Wistar rats were randomly divided into 2 groups: a vehicle group and a GTPs group. Rats in the 2 groups underwent end-to-end neurorrhaphy after the right SN was severed. Subsequently, rats in the vehicle group were intraperitoneally injected with saline for 2 weeks, while those in the GTPs group were intraperitoneally injected with GTPs (50 mg/kg/d, Herbking Biotechnology, Xi'an, China) for 2 weeks.

General observation

At weeks 2, 4, 6, and 8 after establishment of the SNI model in 30 rats, the mental state, activity, healing of the wound, and the occurrence of plantar ulcer in each rat were closely observed, and the color, texture, and adhesion surrounding tissues of the injured SN were also observed. These observations were also made in the 30 rats in the vehicle group.

Neuro-electrophysiological examination

At weeks 2, 4, 6, 8, and 12 after SNI, 6 rats were taken from each time-point in the vehicle group and GTPs group and anesthetized by intraperitoneal injection of 20% uratan (0.6 ml/100 g) prior to neuro-electrophysiological examination. Briefly, the muscle was first separated, and the right SN, tibial nerve, common sural nerve, gastrocnemius, and anterior tibial muscle were exposed. Then, the stimulating electrodes were placed 1.0 cm apart in the proximal end and distal end of the nerve junction, while the recording electrode was obliquely inserted at an angle of 45 degrees into the mid-abdomen in the tibialis anterior muscle. The reference electrode was inserted at the tibialis anterior muscle insertion point, while the grounding electrode was inserted into the tissue between the stimulating electrodes and the recording electrode. The CMAP of rat SN was measured using the CM6240 physiological signal acquisition and processing system (Chengdu Instrument Factory, Chengdu, China), with a frequency of 1 Hz, current of 2 mA, and wave length of 0.2 ms, during which the muscles and nerves were kept moist by saline.

Measurement of tricipital muscle wet weight

To assess the growth rate after nerve transection and anasto-mosis, the tricipital muscle wet weight was measured from the 4th week to 12th week after establishment of the SNI model, with 6 rats for each time-point at weeks 4, 6, 8, and 12 after SNI in the vehicle group and GTPs group. After the neuro-elec-trophysiological examination, the whole tricipital muscle was removed, and the wet weight of the right triceps muscle was weighed using an analytical balance, with the left triceps mus-cle serving as the control. The muscle recovery rate was cal-culated by the following formula: ipsilateral tricipital muscle wet weight/contralateral tricipital muscle wet weight ×100%.

Optical microscopy observation

After the neuro-electrophysiological examination at weeks 2, 4, 6, and 8 after SNI, the distal nerve segment of the anastomot-ic site from 6 rats in the vehicle group and 6 rats in the GTPs group was fixed in glutaraldehyde buffer (pH 7.4, 0.1 mol/L) and 2% osmium tetroxide, dehydrated by a series of etha-nol, and embedded in epoxy resin, successively. Thereafter, the 3-μm semi-thin sections 0.5 cm from the distal end of the nerve anastomosis were stained with toluidine blue, then the regenerated nerve fibers and myelin sheaths were observed. The images were observed under a light microscope (Carl Zeiss, Germany) and 5 random fields were photographed using a col-or digital camera (DC 300F). The total number of myelinated nerve fibers was counted.

Transmission electron microscopy observation

Ultrastructure of the regenerated nerves in SN was observed by transmission electron microscopy using the following pro-tocol. In brief, at week 8 after SNI, samples from 6 rats in the vehicle group and 6 rats in the GTPs group were fixed in glu-taraldehyde buffer (pH 7.4, 0.1 mol/L) and 2% osmium tetrox-ide successively, followed by dehydration with a series of eth-anol, then the samples were embedded in epoxy resin. A Leica UC6 ultra-microtome was used to slice 70-nm ultrathin sec-tions, which were stained by lead and uranium. Eventually, the slices were visualized with a HT 7700 TEM (HITACHI, Japan).

We measured the axonal diameter and myelin sheath thick-ness. The G-ratio was calculated with the followed equation: G-ratio=axonal diameter/axonal diameter+myelin sheath thickness×2.

RT-qPCR

At week 8 after SNI, total RNA was extracted from SN stumps by TRIzol® (Thermo Fisher Scientific, Inc.). RNA concentration was measured by NanoDrop™ 2000 (Thermo Fisher Scientific, Inc.),

followed by reverse-transcription into cDNA by PrimeScript RT Master Mix (Takara Bio, Inc., Otsu, Japan). qPCR was carried out using SYBR Premix Ex Taq (Takara Bio, Inc.) on a CFX96 (Bio-Rad Laboratories). GAPDH was used as an internal refer-ence. Gene expression was analyzed by $2^{-\Delta\Delta Cq}$.

Western blot

At week 8 after SNI, SN stumps were lysed by radioimmunopre-cipitation assay lysis buffer (Beyotime Biotechnology, Shanghai, China) supplemented with protease inhibitor (Sigma-Aldrich). The protein concentration was measured by bicinchonin-ic acid assay (Beyotime Biotechnology) and protein samples (15 μg/lane) were separated by 8% sodium dodecyl sulfate-polyacrylamide gel electrophoresis and transferred to polyvi-nylidene fluoride membranes (Millipore). The membranes were blocked by 5% non-fat milk before incubation with primary antibodies against NGF, GAP-43, NF200, MAG, and GAPDH at 4°C overnight and goat-anti-rabbit peroxidase-conjugated sec-ondary antibody at room temperature for 2 h. Protein bands were visualized by enhanced chemiluminescence detection reagents (Thermo Fisher Scientific, Inc). GAPDH was used as a loading control.

Statistical analysis

Statistical analyses were carried out using SPSS 17.0 (SPSS Software, IBM, USA). Results are expressed as means±standard deviation (SD). Statistical comparisons between 2 groups were performed using the unpaired t test. Differences were consid-ered significant when $P<0.05$.

Results

General situation of rats after SNI

At week 2 after establishment of the SNI model, 30 rats in the vehicle group and 30 rats in the GTPs group exhibited vary-ing degrees of foot/ankle swelling, gait instability, and foot dragging. In addition, in the vehicle group, 3 cases of plan-tar ulcer occurred, which healed at week 7 after SNI, with an obvious scar. However, in the GTPs group, only 1 case of plan-tar ulcer occurred, and the ulcer healed at week 4 after SNI, with a mild scar.

Neurological observation

At week 8 after the establishment of SNI, in 6 rats of the ve-hicle group the SN was hard and extensively adhered to the surrounding tissues, and there were few nutrient vessels on the nerve surface (Figure 1A). However, the 6 rats in the GTPs group had better flexibility and toughness of the SN, less
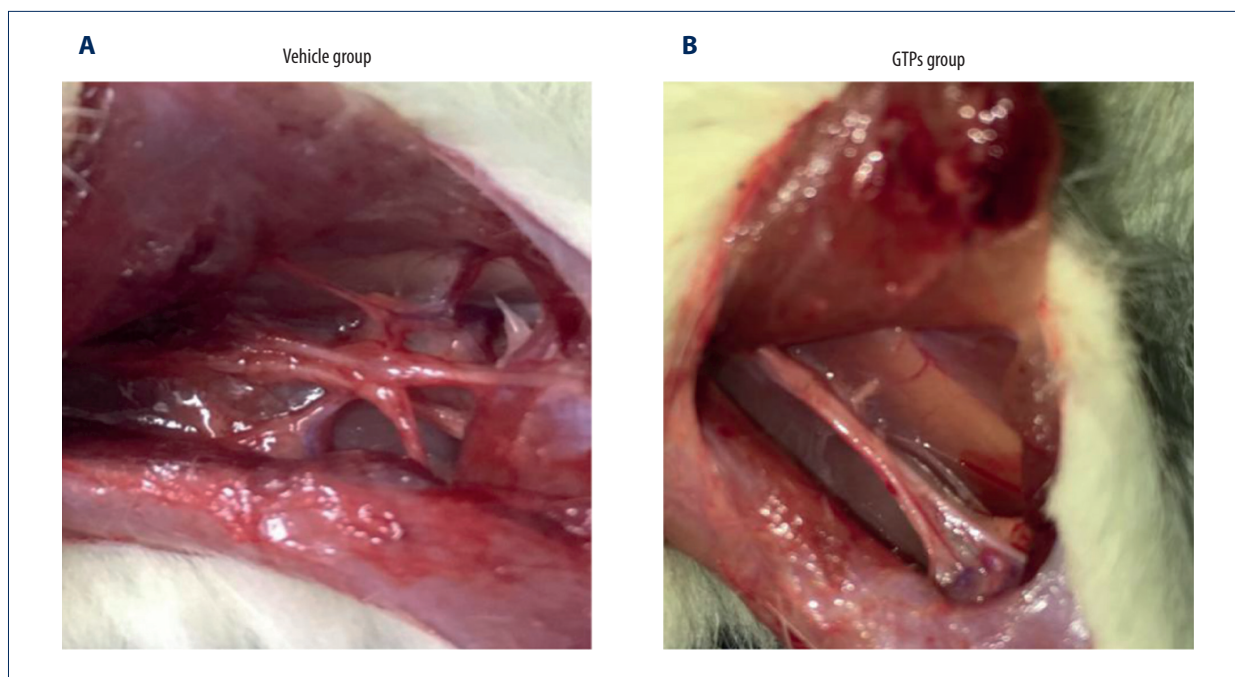
Figure 1. Neurological morphology of SN. The adhesion between nerve anastomosis and surrounding tissues in vehicle group (**A**) and GTPs group (**B**) (n=6).

adhesion to the surrounding soft tissues, and many more nutrient vessels were found on the surface (Figure 1B). In summary, the adhesion between nerve anastomosis and surrounding tissues of rats in the GTPs group was not as serious as in the vehicle group.

Measurement of nerve conduction velocity

At weeks 2, 4, 6, 8, and 12 after SNI, the mean conduction velocity of SN was measured in the vehicle group (n=6) and GTPs group (n=6) (Figure 2). At weeks 2, 4, 6, and 8 after SNI, the mean nerve conduction velocity in the GTPs group was significantly higher than that in the vehicle group ($P<0.01$, Table 1), while at week 12 after SNI, there was no significant difference in nerve conduction velocity between the vehicle group and GTPs group ($P>0.05$, Table 1).

Measurement of wet triceps weight and muscle fiber area

At weeks 4, 8, and 12 after SNI, the muscle recovery rate in the GTPs group was significantly higher than that of the vehicle group ($P<0.01$, Table 2).

Number of myelinated nerve fibers

At week 8 after the establishment of SNI, in the vehicle group (n=6) the morphology of nerve tissue was poor, the main type of regenerated nerve fiber was small-diameter myelinated fiber, the arrangement of myelin sheath was not regular, the maturity

of myelin sheath and axon was somewhat poor, the number and density of myelin sheath and axon were low, and the proliferation of connective tissue was high (Figure 3A). Compared with the vehicle group, the arrangement of regenerated myelinated nerve fibers was more compact, neater, and denser, the diameter of regenerated nerve fibers was larger, and the proliferation of connective tissue was less in the GTPs group (n=6) (Figure 3B).

In addition, the number of myelinated nerve fibers in the GTPs group was significantly higher than that in the vehicle group at weeks 2, 4, 6, and 8 after SNI ($P<0.01$, Table 3), while no significant difference was observed between the vehicle group and GTPs group at week 12 after SNI ($P>0.05$, Table 3).

Ultrastructure of regenerated nerves

At week 8 after the establishment of SNI, in the vehicle group (n=6) the nerve was mainly composed of small and medium-sized myelinated nerve fibers, with sparse, thin, uneven thickness and orderly arrangement of the myelin sheath (Figure 4A). In the GTPs group (n=6) well-developed myelinated nerve fibers occurred, with clear structure, distinct layers, and regular/tight arrangement of myelin sheaths, while the regenerated nerve fibers were slightly uneven in thickness, thin in myelin sheath, and had a moderate number of unmyelinated nerve fibers (Figure 4B). In addition, the corresponding axonal diameter was larger ($P<0.001$), the myelin sheath was thicker ($P<0.001$), and the G-ratio was smaller ($P<0.05$) in the GTPs
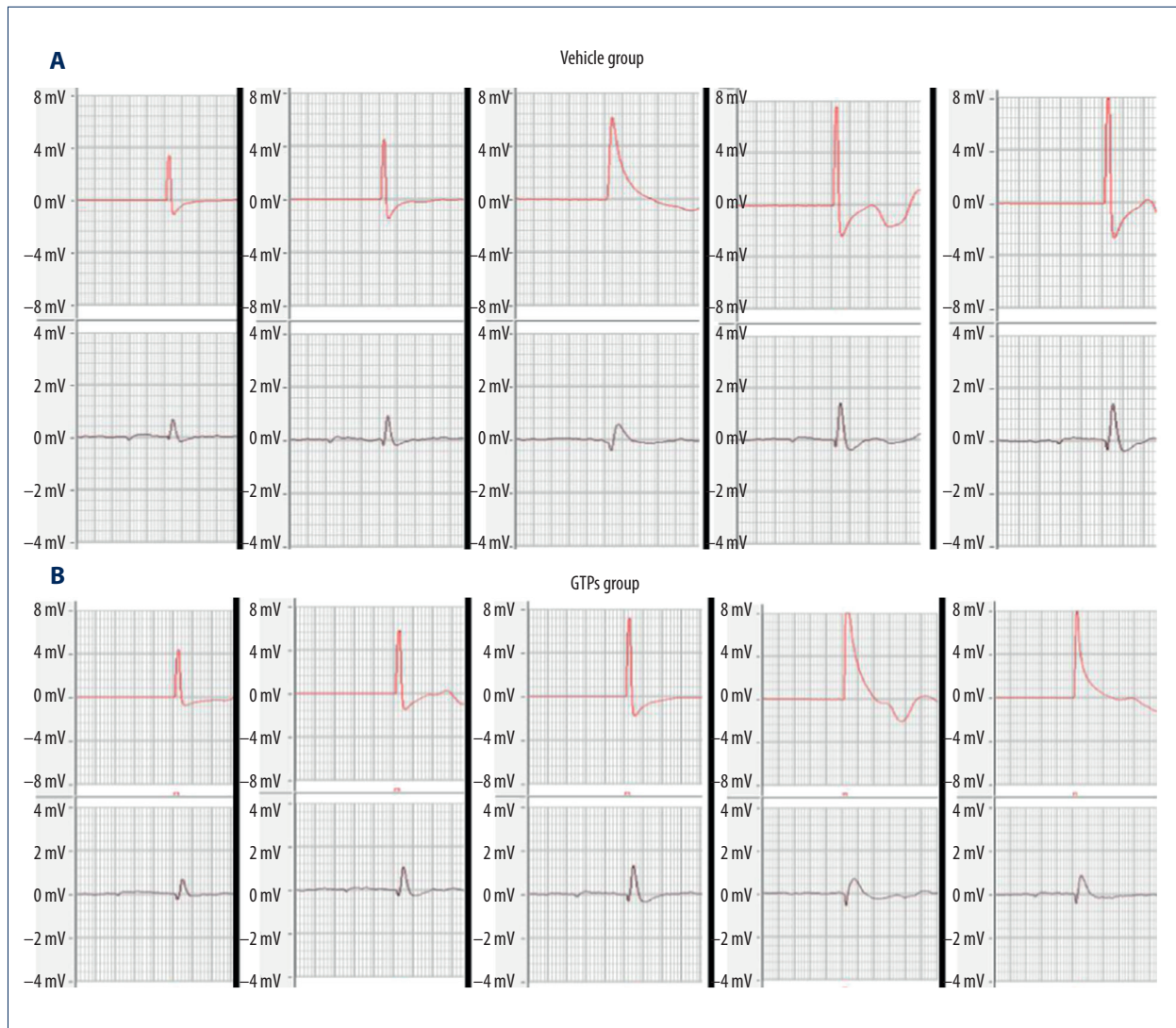
Figure 2. Conduction velocity of SN. At weeks 2, 4, 6, 8, and 12 after SNI, the mean conduction velocity of SN in vehicle group (**A**) and GTPs group (**B**) was measured by CM6240 physiological signal acquisition and processing system (n=6).

Table 1. Nerve conduction velocity at week 2, 4, 6, 8 and 12 after SNI (n=6).

Time	Vehicle group	GTPs group	t	P
Week 2	12.23±1.67	20.54±2.15	7.48	<0.01
Week 4	15.96±3.65	25.13±4.26	4.00	<0.01
Week 6	21.43±4.02	30.23±4.35	3.64	<0.01
Week 8	27.98±4.15	37.66±4.88	3.70	<0.01
Week 12	42.05±5.12	46.98±5.65	1.58	>0.05

Table 2. The recovery rate of wet triceps weight at week 4, 8, 12 after SNI (n=6).

Time	Vehicle group	GTPs group	t	P
Week 4	40.23±4.67	61.54±4.15	8.36	<0.01
Week 8	62.43±5.02	80.23±5.35	5.94	<0.01
Week 12	82.05±5.22	95.98±5.65	4.44	<0.01
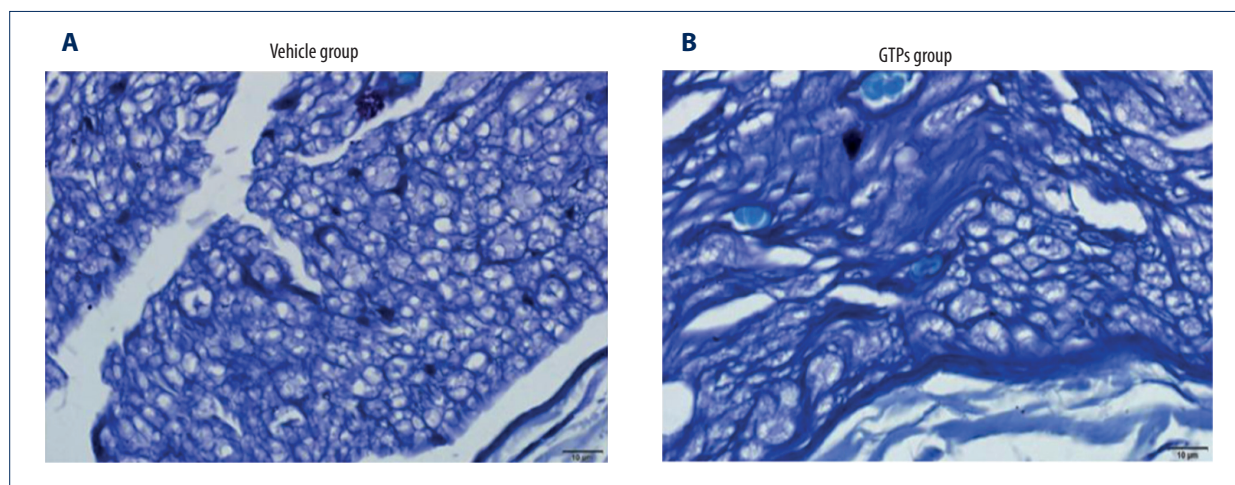
Figure 3. Transverse section of SN. The regenerated nerve fibers and myelin sheaths in vehicle group (**A**) and GTPs group (**B**) were measured by optical microscopy (n=6).

Table 3. Number of myelinated nerve fibers at week 2, 4, 6, 8 and 12 after SNI (n=6).

Time	Vehicle group (10^4)	GTPs group (10^4)	t	P
Week 2	45.22±3.66	60.24±4.45	6.39	<0.01
Week 4	50.66±4.36	76.87±5.03	9.64	<0.01
Week 6	70.36±6.23	98.75±6.89	7.49	<0.01
Week 8	89.35±8.45	118.95±8.59	6.02	<0.01
Week 12	140.00±8.21	150.00±8.27	2.10	>0.05

group than in the vehicle group (Table 4). These results show that nerve regeneration in the GTPS group was significantly better than in the vehicle group.

Underlying molecules in SN stumps

At week 8 after the establishment of SNI, expression of NGF, GAP-43, NF200, and MAG in SN stumps was significantly higher in the GTPs group (n=6) than in the vehicle group (n=6) (Figure 5A–5C).

Discussion

PNI accounts for approximately 1.5–4.0% of the world's annual new trauma cases [1]. Many drug-based treatments have been explored for PNI repair. For instance, 4-AP promotes recovery of acute PNI and myelin regeneration in rats [2], vitamin supplements are beneficial for nerve regeneration in acute PNI [5], genistein is an adjuvant therapy for PNI [11], and these effects may be related to changes in estrogen level [12]. However, adverse effects exist, and there is an urgent need to find a convenient and accessible treatment without adverse effects.

GTPs in green tea exhibit protective effects in the CNS. For instance, GTPs prevent brain degenerative diseases [9,13,14] and
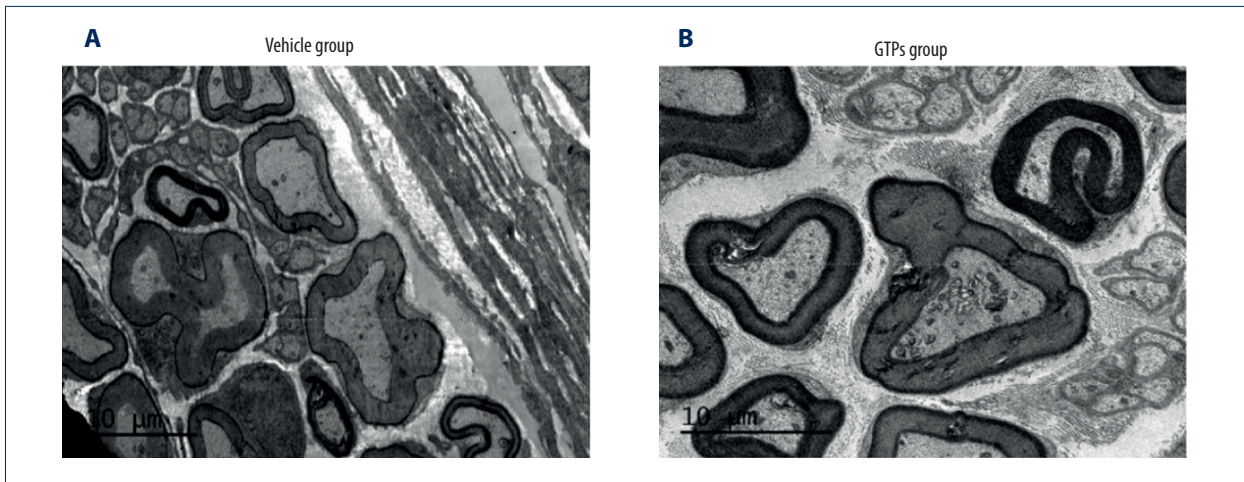
Figure 4. Ultrastructure of regenerated nerves in SN. The regenerated nerves in vehicle group (**A**) and GTPs group (**B**) were tested by a transmission electron microscopy (n=6).

Table 4. Ultrastructure of regenerated nerves at week 8 after SNI (n=6).

Group	Vehicle group	GTPs group	t	P
Axonal diameter (µm)	4.56±0.28	5.81±0.28	7.82	<0.001
myelin sheath thickness (µm)	2.15±0.08	3.09±0.04	27.94	<0.001
G-ratio	0.51±0.02	0.48±0.01	3.10	<0.05
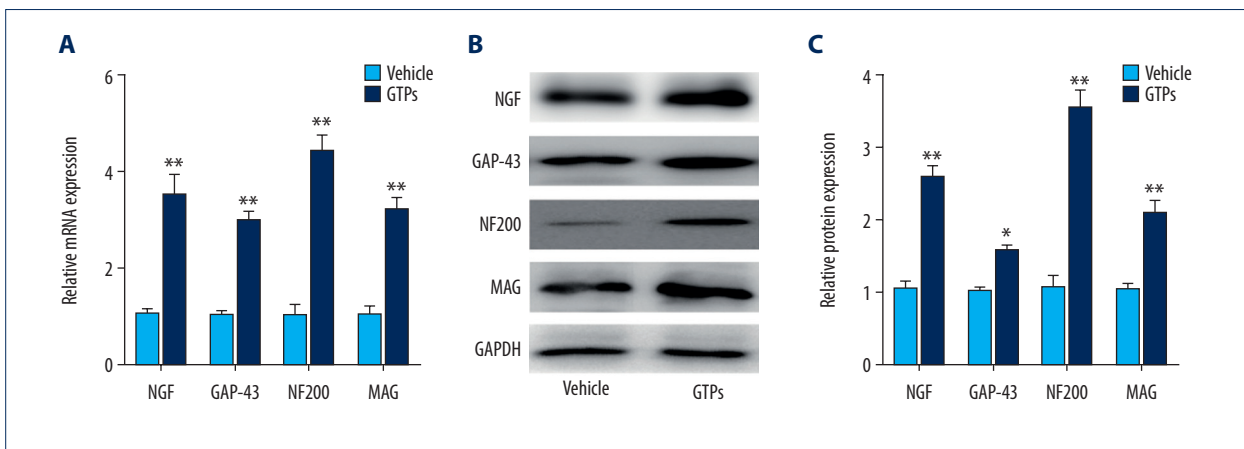
Figure 5. Underlying molecules in SN stumps. Expression of NGF, GAP-43, NF200, and MAG in SN stumps in vehicle group and GTPs group (**A–C**) was measured by RT-qPCR and Western blot (n=6). *P*<0.01, GTPs group *vs.* vehicle group.

cerebral ischemic diseases [15]. In addition, GTPs reduce the immune response and injury of transplanted PN in rats [16]; and (-)-epigallocatechin gallate (EGCG) in GTPs improves the survival of motor neurons after PNI [17]. The effects of GTPs on the PNS have not been previously investigated, and the present study aimed to determine whether GTPs can promote nerve regeneration in rats after PNI. The concentration of GTPs was first explored prior to performing the present study. Low and medium doses of GTPs are beneficial for hepatotoxicity

and nephrotoxicity [18], while high doses of GTPs cause hepatotoxicity [19], which agrees with our initial preliminary work (data not shown) in which 3 doses of GTPs were tested: 50 mg/kg/d, 100 mg/kg/d, and 200 mg/kg/d. However, 1 rat died in the 100 mg/kg/d dosage group, and all rats died in the 200 mg/kg/d dosage group, due to respiratory tract disease, digestive tract disease, and eye congestion. All rats in the 50 mg/kg/d dosage group survived; thus, it was chosen for use in the subsequent experiments.

GTPs not only reduces lymphocyte production of pro-inflammatory cytokines, but also reduces inflammation around trauma [7]. Overexpression of inflammatory mediators in osteoarthritis can be inhibited by EGCG in GTPs [20]. GTPs also increase the production of vascular endothelial factors [21]. The present study found less adhesion between nerves and surrounding tissues at anastomotic stoma in the GTPs group than in the vehicle group, which may be due to the anti-inflammatory effects of GTPs; additionally, GTPs promote the regeneration of blood vessels around the injury, which may be responsible for the abundant capillaries around the nerve anastomosis. The slight inflammation in nerve anastomosis in the GTPs group may be related to the anti-inflammation effects of GTPs [22–24].

GTPs not only reduce blood sugar and lipids by inhibiting appetite and nutrient absorption, but also participate in lipid metabolism by regulating glycogen and lipid synthesis enzymes in the liver [25]. Furthermore, it can even change the expression of obesity genes of rats [26]. Nerve regeneration after PNI depends on recovery of limb function, and the nerve growth rate is a key factor affecting muscular atrophy [2]. In the present study the weight gain was slower and the recovery rate of wet triceps weight and nerve conduction velocity were faster in the GTPs group, indicating that GTPs stimulate nerves, promote the recovery from muscle atrophy, and improve the activity of affected limbs, despite its inhibitory effects on appetite and fat synthesis in rats.

Cells that function in nerve regeneration attracted our attention. Schwann cells (SCs) are precursor cells with reversible differentiation and different morphologies/functions, consisting of myelin- and non-myelin-forming cells [27]. In addition, SCs synthesize and secrete various NGF, neurotrophic factor (NTF), nerve cell adhesion factor (NCAF), and basement membrane adhesion proteins [28,29]. SCs play an important role in nerve regeneration [30]. For instance, at the axotomy of the CNS, most axons of the implanted SCs grow rapidly into the distal nerve of the graft, whose growth direction is consistent with the arrangement of SCs [31]. The present study found that nerve recovery in the GTPs group was much faster than that in the vehicle group, regardless of the number of myelinated nerve fibers, thickness of the myelin sheath, and morphology of SCs. The underlying mechanisms responsible for the effects of GTPs remain to be investigated. GAP-43 is a specific protein expressed during nerve regeneration and its high expression is associated with active nerve regeneration [32]. As one of the 6 growth factors, NGF functions in the survival and differentiation of neurons in the CNS [33] and its expression is increased in Schwann cells during nerve regeneration [34]. MAG is involved in the formation and maintenance of myelin [35], and NF200 is a marker of myelinated neurons [36]. The expression of NGF, GAP-43, NF200, and MAG in SN stumps was observed to be higher in the GTPs group than in the vehicle group.

Interestingly, there are also other agents applied for treatment of PNI. For instance, quercetin induces neurite growth by promoting GAP-43 expression [37], and isoquercitrin promotes peripheral nerve regeneration and remyelination after sciatic crush injury in mice [38]. The effects of GTPs on peripheral nerve regeneration and remyelination are similar to those of isoquercitrin.

In rats with SNI, GTPs relieved the adhesion between nerve anastomosis and surrounding tissues and improved the muscle recovery rate. At weeks 2, 4, 6, and 8 after SNI, the mean nerve conduction velocity and the number of myelinated nerve fibers in the GTPs group were higher than those in the vehicle group, while there was no significant difference at week 12 after SNI, which suggests that SN regeneration had occurred by week 12 after SNI in rats, and this effect warrants further study.

Conclusions

The present study demonstrated that GTPs promote recovery from PNI.

Conflict of interests

None.

This work is licensed under Creative Common Attribution-
NonCommercial-NoDerivatives 4.0 International (CC BY-NC-ND 4.0)

e923806-8

Indexed in: [Current Contents/Clinical Medicine] [SCI Expanded] [ISI Alerting System]
[ISI Journals Master List] [Index Medicus/MEDLINE] [EMBASE/Excerpta Medica]
[Chemical Abstracts/CAS]

References:

1. Siemionow M, Brzezicki G: Current techniques and concepts in peripheral nerve repair. Int Rev Neurobiol, 2009; 87: 141–72

2. Tseng KC, Li HY, Clark A et al: 4-Aminopyridine promotes functional recovery and remyelination in acute peripheral nerve injury. Embo Mol Med, 2016; 8: 1409–20

3. Mandelbaum-Livnat MM, Almog M, Nissan M et al: Photobiomodulation triple treatment in peripheral nerve injury: Nerve and muscle response. Photomed Laser Surg, 2016; 34: 638–45

4. Nan JN, Hu XG, Li HX et al: Use of nerve conduits for peripheral nerve injury repair A Web of Science-based literature analysis. Neural Regen Res, 2012; 7: 2826–33

5. Altun I, Kurutas EB: Vitamin B complex and vitamin B-12 levels after peripheral nerve injury. Neural Regen Res, 2016; 11: 842–45

6. Bornhoeft J, Castaneda D, Nemoseck T et al: The protective effects of green tea polyphenols: Lipid profile, inflammation, and antioxidant capacity in rats fed an atherogenic diet and dextran sodium sulfate. J Med Food, 2012; 15: 726–32

7. Molina N, Bolin AP, Otton R: Green tea polyphenols change the profile of inflammatory cytokine release from lymphocytes of obese and lean rats and protect against oxidative damage. Int Immunopharmacol, 2015; 28: 985–96

8. Li YY, Buckhaults P, Cui XQ et al: Combinatorial epigenetic mechanisms and efficacy of early breast cancer inhibition by nutritive botanicals. Epigenomics, 2016; 8: 1019–37

9. Mandel SA, Amit T, Kalfon L et al: Targeting multiple neurodegenerative diseases etiologies with multimodal-acting green tea catechins. J Nutr, 2008; 138: 1578–83

10. Liu XB, Wang ZH, Wang P et al: Green tea polyphenols alleviate early BBB damage during experimental focal cerebral ischemia through regulating tight junctions and PKCalpha signaling. BMC Complem Altern Med,. 2013; 13: 187

11. Ozbek Z, Aydin HE, Kocman AE et al: Neuroprotective effect of genistein in peripheral nerve injury. Turk Neurosurg, 2017; 27: 816–22

12. Altun I, Kurutas EB: G protein-coupled estrogen receptor levels after peripheral nerve injury in an experimental rat model. World Neurosurg, 2015; 84: 1903–6

13. Mandel SA, Amit T, Weinreb O et al: Understanding the broad-spectrum neuroprotective action profile of green tea polyphenols in aging and neurodegenerative diseases. J Alzheimers Dis, 2011; 25: 187–208

14. Nie G, Cao Y, Zhao B: Protective effects of green tea polyphenols and their major component, (-)-epigallocatechin-3-gallate (EGCG), on 6-hydroxydopamine-induced apoptosis in PC12 cells. Redox Rep, 2002; 7: 171–77

15. Lee S, Suh S, Kim S: Protective effects of the green tea polyphenol (-)-epigallocatechin gallate against hippocampal neuronal damage after transient global ischemia in gerbils. Neurosci Lett, 2000; 287: 191–94

16. Ikeguchi R, Kakinoki R, Okamoto T et al: Successful storage of peripheral nerve before transplantation using green tea polyphenol: An experimental study in rats. Exp Neurol, 2003; 184: 688–96

17. Wei IH, Tu HC, Huang CC et al: (-)-Epigallocatechin gallate attenuates NADPH-d/nNOS expression in motor neurons of rats following peripheral nerve injury. BMC Neurosci, 2011; 12: 52

18. Inoue H, Maeda-Yamamoto M, Nesumi A et al: Low and medium but not high doses of green tea polyphenols ameliorated dextran sodium sulfate-induced hepatotoxicity and nephrotoxicity. Biosci Biotechnol Biochem, 2013; 77: 1223–28

19. Murakami A: Dose-dependent functionality and toxicity of green tea polyphenols in experimental rodents. Arch Biochem Biophys, 2014; 557: 3–10

20. Oliviero F, Sfriso P, Scanu A et al: Epigallocatechin-3-gallate reduces inflammation induced by calcium pyrophosphate crystals *in vitro*. Front Pharmacol, 2013; 4: 51

21. Heber D, Zhang Y, Yang J et al: Green tea, black tea, and oolong tea polyphenols reduce visceral fat and inflammation in mice fed high-fat, high-sucrose obesogenic diets. J Nutr, 2014; 144: 1385–93

22. Ramasamy C: Potential natural antioxidants: Adjuvant effect of green tea polyphenols in periodontal infections. Infect Disord Drug Targets, 2015; 15: 141–52

23. Chen L, Mo H, Zhao L et al: Therapeutic properties of green tea against environmental insults. J Nutr Biochem, 2017; 40: 1–13

24. Hsu S: Compounds derived from epigallocatechin-3-gallate (EGCG) as a novel approach to the prevention of viral infections. Inflamm Allergy Drug Targets, 2015; 14: 13–18

25. Kim JJ, Tan Y, Xiao L et al: Green tea polyphenol epigallocatechin-3-gallate enhance glycogen synthesis and inhibit lipogenesis in hepatocytes. Biomed Res Int, 2013; 2013: 920128

26. Lu C, Zhu W, Shen CL et al: Green tea polyphenols reduce body weight in rats by modulating obesity-related genes. PLoS One, 2012; 7: e38332

27. Jessen KR, Mirsky R: Origin and early development of Schwann cells. Microsc Res Techniq, 1998; 41: 393–402

28. Dubovy P: Schwann cells and endoneurial extracellular matrix molecules as potential cues for sorting of regenerated axons: A review. Anat Sci Int, 2004; 79: 198–208

29. Johnson EO, Zoubos AB, Soucacos PN: Regeneration and repair of peripheral nerves. Injury, 2005; 36: S24–29

30. Dezawa M, Kawana K, Adachi-Usami E: The role of Schwann cells during retinal ganglion cell regeneration induced by peripheral nerve transplantation. Invest Ophthalmol Vis Sci, 1997; 38: 1401–10

31. Bravin M, Savio T, Strata P et al: Olivocerebellar axon regeneration and target reinnervation following dissociated Schwann cell grafts in surgically injured cerebella of adult rats. Eur J Neurosci, 1997; 9: 2634–49

32. Gordon T, Tetzlaff W: Regeneration-associated genes decline in chronically injured rat sciatic motoneurons. Eur J Neurosci, 2015; 42: 2783–91

33. Dai CF, Steyger PS, Wang ZM et al: Expression of Trk A receptors in the mammalian inner ear. Hearing Res, 2004; 187: 1–11

34. Karahan G, Kaya H, Erdogan MA et al: Effects of trimetazidine on nerve regeneration in a rat sciatic nerve injury model. Bratisl Lek Listy, 2019; 120: 777–82

35. Pronker MF, Lemstra S, Snijder J et al: Structural basis of myelin-associated glycoprotein adhesion and signalling. Nat Commun, 2016; 7: 13584

36. Drummond ES, Dawson LF, Finch PM et al: Increased bilateral expression of alpha1-adrenoceptors on peripheral nerves, blood vessels and keratinocytes does not account for pain or neuroinflammatory changes after distal tibia fracture in rats. Neuroscience, 2014; 281: 99–109

37. Chen MM, Yin ZQ, Zhang LY et al: Quercetin promotes neurite growth through enhancing intracellular cAMP level and GAP-43 expression. Chin J Nat Med, 2015; 13: 667–72

38. Qiu J, Yang X, Wang L et al: Isoquercitrin promotes peripheral nerve regeneration through inhibiting oxidative stress following sciatic crush injury in mice. Ann Transl Med, 2019; 7: 680